JOURNAL OF Materials CHEMISTRY

Thermoelectric properties of highly textured $(ZnO)_5In_2O_3$ ceramics

Toshihiko Tani,*[a] Shinya Isobe,[b] Won-Seon Seo[b]† and Kunihito Koumoto[b]

[a]*Toyota Central R&D Labs., Inc., Nagakute, Aichi, 480-1192, Japan. E-mail: toshit@mosk.tytlabs.co.jp*
[b]*Department of Applied Chemistry, Graduate School of Engineering, Nagoya University, Nagoya 464-8603, Japan*

Received 14th February 2001, Accepted 7th June 2001
First published as an Advance Article on the web 30th July 2001

Textured bulk ceramics of the layer-structured homologous compound $(ZnO)_5In_2O_3$ were fabricated by the reactive templated grain growth (RTGG) technique and the thermoelectric properties evaluated. Plate-like $ZnSO_4{\cdot}3Zn(OH)_2$ particles were mixed with In_2O_3 powders and the mixture was tape cast to form a sheet, such that the $ZnSO_4{\cdot}3Zn(OH)_2$ platelets were aligned parallel to the sheet surface; the sheets were then sintered to form a single phase of $(ZnO)_5In_2O_3$ with the *c*-axis perpendicular to the sheet surface. The electrical conductivity, σ, was found to be highly anisotropic in the textured specimen; that is, σ (in the *ab*-plane) $> \sigma$ (along the *c*-axis). The textured specimen shows a porous microstructure and exhibits lower thermal conductivity than a dense ceramic specimen with random orientation. As a result, the thermoelectric figure of merit of the textured $(ZnO)_5In_2O_3$ specimen is nearly three times as large as that of the randomly oriented specimen.

1 Introduction

Homologous compounds of the form $(ZnO)_kIn_2O_3$ (k = an integer > 3) are candidate base materials for high temperature thermoelectric energy conversion.[1] These compounds have very unusual crystal structures, belonging to the space groups $R3m$ (for k = odd) or $P6_3/mmc$ (for k = even) and are composed of layers of $InO_{3/2}$, $InZnO_{5/2}$, and ZnO, which are stacked sequentially along the *c*-axis of the hexagonal system.[2] They show n-type semiconducting behavior induced by certain deviations from stoichiometric compositions.[1,3] Investigation of sputter-deposited $(ZnO)_5In_2O_3$ thin films with preferred orientations revealed that the electrical conductivity of the compound is highly anisotropic, in spite of the orientation-independent characteristics of the Seebeck coefficient.[4] This suggested that the carrier mobility of $(ZnO)_5In_2O_3$ along the *ab*-plane (basal plane) of a hexagonal lattice is larger than that across the *ab*-plane; furthermore, highly textured bulk ceramics would exhibit higher thermoelectric figures of merit than randomly oriented ceramics with the same composition.

There are two well-known methods which predominate for the preparation of textured oxide ceramics; one is hot forging and the other is sintering of aligned particles with anisotropic shapes. In the former method, grains are aligned parallel to a slip plane by the application of pressure near sintering temperatures.[5,6] In the latter, grain alignment is enhanced by anisotropic grain growth; the templated grain growth (TGG) and reactive templated grain growth (RTGG) techniques have been developed to obtain highly textured ceramics more easily than using the pressure induced method.[7–10] In particular, the essential difference between TGG and RTGG is whether the template particles react during firing. With RTGG, reactive template particles are mixed with the other ingredients and aligned by tape casting or extrusion. During heat treatment, the product material is formed *in situ* with the orientation of the template being preserved.[8,10,11] Thus the RTGG technique is considered to be sufficiently flexible for the preparation of textured oxide ceramics if a suitable template material is available. In this paper, we report structural and thermoelectric properties of textured $(ZnO)_5In_2O_3$ ceramics prepared by the RTGG technique using plate-like $ZnSO_4{\cdot}3Zn(OH)_2$.

2 Experimental

2.1 Characterization of the reactive template

Plate-like $ZnSO_4{\cdot}3Zn(OH)_2$ particles (Hakusui Tech Co.), with particle sizes of 2–10 μm and thicknesses of 0.1–0.3 μm (see Fig. 1), were used as the reactive template. Both thermogravimetric and powder X-ray diffraction (XRD) analyses were conducted to investigate the thermal decomposition characteristics of the template particles. A powdered mixture of $ZnSO_4{\cdot}3Zn(OH)_2$ and In_2O_3 (Kojundo Chemical Laboratory Co.; purity: 99.99%; average particle size: 1 μm) with a molar ratio of Zn : In = 5 : 2 was heat treated at 1423 K for 6 h in air and the changes in the shape and phase of the template particles were examined by SEM and XRD.

2.2 Preparation of textured $(ZnO)_5In_2O_3$ ceramics

$ZnSO_4{\cdot}3Zn(OH)_2$ platelets and In_2O_3 powder were combined in a molar ratio of Zn : In = 5 : 2 and mixed with a solvent (60%

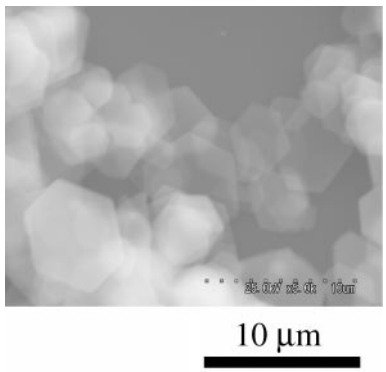

Fig. 1 SEM image of plate-like $ZnSO_4{\cdot}3Zn(OH)_2$ particles used as the reactive template for textured $(ZnO)_5In_2O_3$ ceramics.

†Present address: Korea Institute of Ceramic Engineering & Technology, Seoul, Korea.

 DOI: 10.1039/b101474i

toluene–40% ethanol, v/v) in a ball mill for 4 h. Binder [poly(vinyl butyral)] and plasticizer (di-n-butyl phthalate) were added and the mixture milled for another hour. The slurry was tape cast to form a sheet with a thickness of *ca.* 0.2 mm. The sheet was cut, stacked, and pressed at 10 MPa for 10 min at 80 °C to form billets 10 mm thick. The billets were heated at 1423 K for 6 h in air to form $(ZnO)_5In_2O_3$. After cold isostatic pressing, the specimens were sintered at 1823 K for 2 h in air (denoted as RTGG-processed specimen).

A reference specimen with random grain orientation was also prepared by conventional powder processing. A mixed-powder compact of ZnO and In_2O_3 with the same Zn : In ratio as the RTGG-processed specimen was heat treated at 1423 K for 6 h in air to form $(ZnO)_5In_2O_3$. Pulverized $(ZnO)_5In_2O_3$ was packed by cold isostatic pressing and the compact specimen was sintered at 1823 K for 2 h in air (denoted as REF specimen).

Crystalline phases and the degree of orientation were determined by XRD analysis with Cu-Kα radiation of the two sintered specimens. For the RTGG-processed specimens, texture development was examined on the polished surfaces parallel (denoted as ∥surface) and perpendicular (denoted as ⊥surface) to the original sheet plane, as compared to the reference specimen. The degree of orientation, F, was calculated from eqns. (1)–(3) (Lotgering method).[12]

$$F = (P - P_0)/(1 - P_0) \quad (1)$$

$$P = \Sigma I_{(00l)}/\Sigma I_{(hkl)} \quad (2)$$

$$P_0 = \Sigma I_{0(00l)}/\Sigma I_{0(hkl)} \quad (3)$$

where I and I_0 are the diffraction intensities for textured and randomly oriented specimens, respectively, and (00l) and (hkl) stand for the Miller indices. The diffraction lines between $2\theta = 10$ and 80° were used to calculate P and P_0.

Microstructures were observed by SEM for the RTGG-processed specimen on the sintered surfaces parallel and perpendicular to the original sheet plane. Fracture surfaces were also observed by SEM for the RTGG-processed and REF specimens.

Rectangular bars were machined out of the RTGG-processed specimen for the measurement of electrical conductivity (σ) and Seebeck coefficient (α), so that the bars were parallel (denoted as ∥specimen) and perpendicular (denoted as ⊥specimen) to the original sheet plane, as shown in Fig. 2. Disc specimens were also made with their axes parallel (∥specimen) and perpendicular (⊥specimen) to the original sheet plane, for the measurement of thermal conductivity (κ). Rectangular and disc specimens were similarly machined out of the REF material for the thermoelectric property measurements.

2.3 Measurement of properties

Electrical conductivity and thermopower were measured simultaneously at 673 to 1073 K under Ar atmosphere. Electrical conductivity was measured by the dc 4-probe method by using each Pt leg of the thermocouple as a current lead. Two more Pt leads wound around the specimen were used to measure the voltage drop. An average σ value was taken for four consecutive measurements with different current density after the deviation in the four values became within 1%. For the thermopower measurements, a temperature gradient in the specimen was generated by passing cool air through a hollow quartz tube placed near one end of the specimen. The temperature difference between the two ends was controlled to be 2 to 15 K by varying the flow rate of the air. Five thermoelectric power data points measured as a function of temperature difference gave a straight line and the Seebeck coefficient was calculated from its slope.

Thermal diffusivity was measured by the laser flash method (ULVAC, TC-3000V) and specific heat capacity was measured by a differential scanning calorimeter (TA Instruments, MDSC 2910). Thermal conductivity (κ) was calculated from thermal diffusivity (β), specific heat capacity (C_p), and density (ρ), according to the equation:

$$\kappa = \beta C_p \rho \quad (4)$$

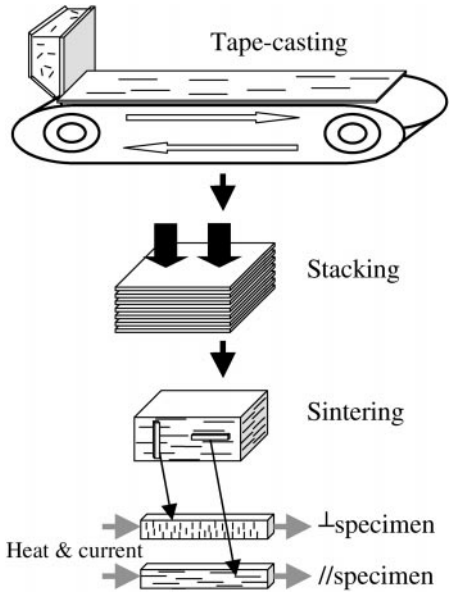

Fig. 2 A schematic representation of the preparative method employed to obtain textured $(ZnO)_5In_2O_3$ ceramics and specimens for thermoelectric property measurements.

3 Results and discussion

3.1 Characterization of the reactive template

The crystal structure of the $ZnSO_4 \cdot 3Zn(OH)_2$ belongs to the hexagonal system and XRD analysis confirms that the *ab*-plane is parallel (*c*-axis is perpendicular) to the developed plane of the plate-like particles. Fig. 3 shows the results of thermogravimetric analysis of the $ZnSO_4 \cdot 3Zn(OH)_2$ particles when heated at 10 K min^{-1}. Two decomposition stages were found during heating:

$$393-473\ \text{K: } ZnSO_4 \cdot 3Zn(OH)_2 \rightarrow (5/2)ZnO + (1/2)ZnO \cdot 2ZnSO_4 + 3H_2O\uparrow \quad (5)$$

$$873-973\ \text{K: } 2ZnO \cdot 2ZnSO_4 \rightarrow 3ZnO + 2SO_3\uparrow \quad (6)$$

Fig. 4 shows SEM images of the particles after heating at 873, 1073, and 1273 K. The mixed-phase particle of ZnO with $ZnO \cdot 2ZnSO_4$ (873 K) maintained the hexagonal plate-like shape of the original. After heating at 1073 K, many through-holes were observed on the hexagonal ZnO particles, and the original shape was completely lost after heating at 1273 K. For the powder mixture of $ZnSO_4 \cdot 3Zn(OH)_2$ and In_2O_3, however,

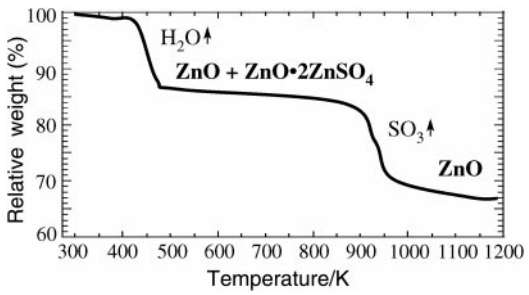

Fig. 3 The result of thermogravimetric analysis of the plate-like $ZnSO_4 \cdot 3Zn(OH)_2$ particles.

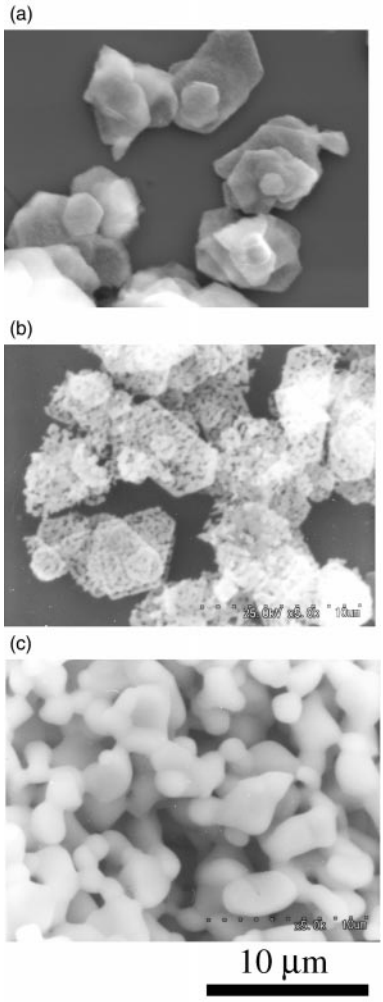

Fig. 4 SEM images of plate-like $ZnSO_4 \cdot 3Zn(OH)_2$ particles after heat treatment at (a) 873, (b) 1073, and (c) 1273 K.

the hexagonal plate-like shape was still preserved, even after heating at 1423 K for 6 h, as shown in Fig. 5. XRD analysis identified the plate-like particles as homologously structured $(ZnO)_5In_2O_3$ with the *c*-axis perpendicular to the developed plane. This result supports the feasibility of texture design by the use of the plate-like particles as a reactive template.

3.2 Texture development

Fig. 6 shows the XRD patterns of the RTGG-processed ceramics sintered at 1823 K with different irradiation directions, the reference pattern being that of the REF specimen. Single-phase $(ZnO)_5In_2O_3$ was formed, except for the surface layer which contained byproducts such as $(ZnO)_3In_2O_3$ and $(ZnO)_{19}In_2O_3$. The ‖surface exhibits high diffraction intensities

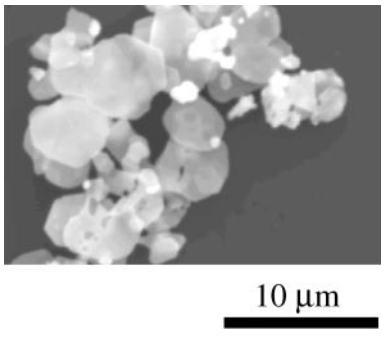

Fig. 5 SEM image of plate-like $ZnSO_4 \cdot 3Zn(OH)_2$ particles mixed with In_2O_3 after heat-treatment at 1423 K for 6 h.

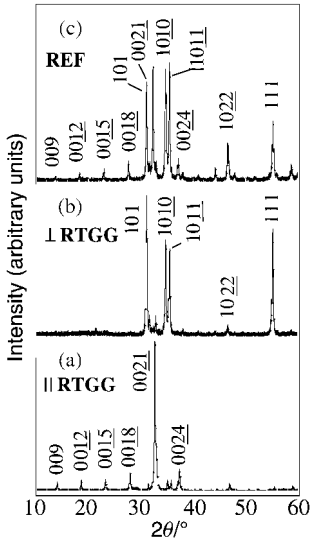

Fig. 6 XRD patterns of textured specimens for polished surfaces (a) parallel and (b) perpendicular to the sheet plane, compared with (c) the pattern for the REF specimen used as a reference.

for the *ab*-planes of $(ZnO)_5In_2O_3$, whereas the diffraction lines of the $\{00l\}$ planes are hardly observed for the ⊥surface. The degree of $\{00l\}$ orientation, F, for the ‖surface reached 0.80. The texture also developed at lower temperatures, and the RTGG-processed specimen exhibited a degree of orientation as high as 0.78 after heat treatment at 1423 K.

Fig. 7 shows SEM images for sintered surfaces of the RTGG-processed specimens in comparison with the REF specimen. The SEM image of the ⊥surface reveals a unique microstructure with plate-like grains piled up in the direction perpendicular to the sheet plane while the ‖surface image shows the developed surfaces of the plate-like grains. The results of the microstructure observation also confirm the development of uniaxial texture, which is typical of layer-structured compounds with grain orientation. The relative density of the RTGG-processed specimen is approximately 90% of that of $(ZnO)_5In_2O_3$ whereas the density of the REF specimen is as expected. Fracture surfaces of the sintered specimens are compared in Fig. 8. Many pores of 5–10 μm in size are observed for the RTGG-processed specimen.

3.3 Thermoelectric properties

Fig. 9 shows the temperature dependence of the electrical conductivity, σ, for the three specimens. The ‖specimen exhibits electrical conductivity similar to that of the REF specimen, even though the RTGG-processed specimen has a density 10% lower than that of the conventionally processed REF specimen. The ‖specimen shows higher electrical conductivity than the ⊥specimen. The difference in electrical conductivity between the two specimens is, however, smaller than expected from the results observed for the thin films.[4] The smaller differences in σ between the two directions for the RTGG-processed specimen can be attributed to the misalignment distribution in the textured polycrystal.

Fig. 10 shows the Seebeck coefficient, α, as a function of temperature. Although the temperature-dependent values are in the order $|\alpha$ (‖specimen)$| > |\alpha$ (REF)$| > |\alpha$ (⊥specimen)$|$, the differences are relatively small.

Fig. 11 shows the temperature dependence of the thermal conductivity, κ. The κ values of the RTGG-processed specimen are more than 60% smaller than those for the REF specimen, regardless of the direction of measurment. The lower density of the RTGG-processed specimen accounts for the lower κ compared to the more dense REF specimen.

The thermoelectric figure of merit, $Z = \alpha^2\sigma/\kappa$, was calculated

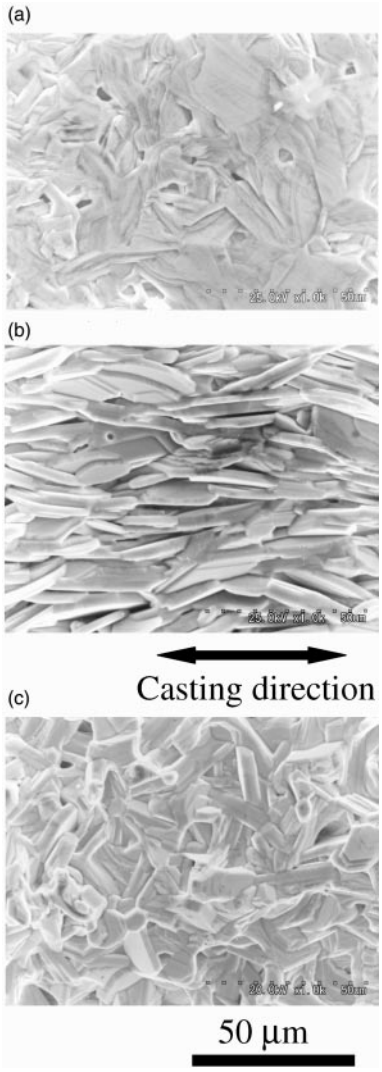

Fig. 7 SEM images of sintered surfaces (a) parallel and (b) perpendicular to the sheet plane for the RTGG-processed $(ZnO)_5In_2O_3$ ceramics, compared with (c) a sintered surface of the REF specimen.

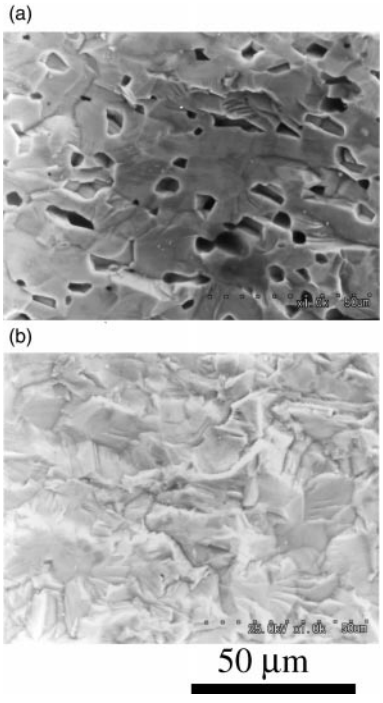

Fig. 8 SEM images of fracture surfaces for the (a) RTGG-processed and (b) REF specimens.

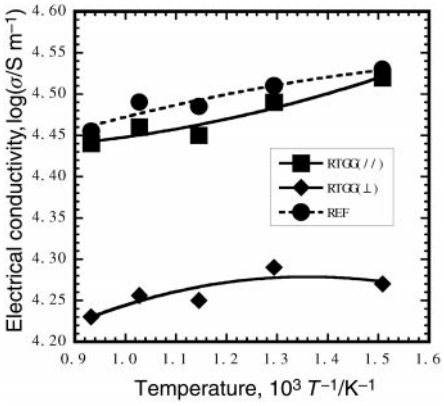

Fig. 9 Temperature dependence of the electrical conductivity (σ) for textured and reference specimens.

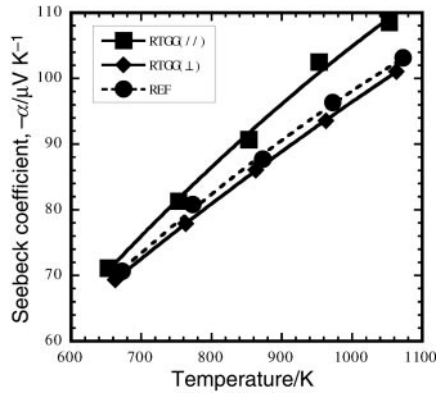

Fig. 10 Temperature dependence of the Seebeck coefficient (α) for textured and reference specimens.

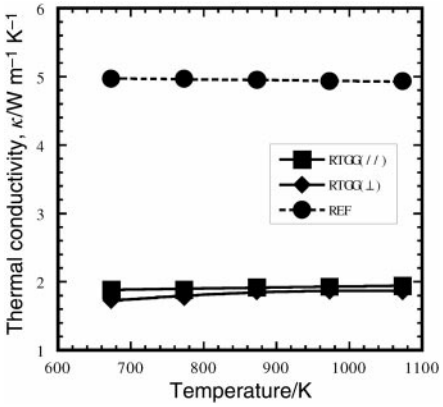

Fig. 11 Temperature dependence of the thermal conductivity (κ) for textured and reference specimens.

and is shown in Fig. 12. The ∥specimen, in which electrical and thermal fluxes are presumed to be parallel to the preferential *ab*-plane, exhibits higher Z values than the ⊥specimen, in which electrical and thermal fluxes are parallel to the preferential *c*-axis, as expected. The relative difference in the Z values between the two directions was 62–86% in the present temperature range. Both sets of Z values for the RTGG-processed specimen are higher than those of the REF specimen because of the lower thermal conductivity. The ∥specimen exhibits Z values 2.5–2.7 times as high as the REF specimen. The highest Z and ZT values in the measurement temperature range are $1.7 \times 10^{-4}\ K^{-1}$ and 0.18 (at 1073 K), respectively.

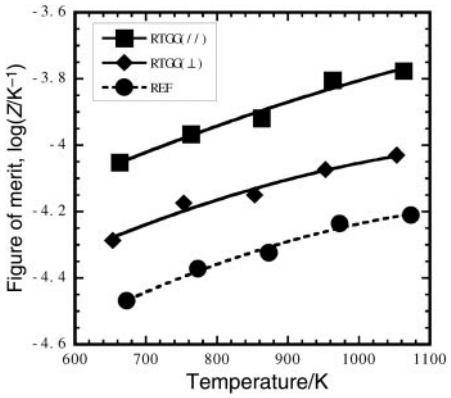

Fig. 12 Temperature dependence of the thermoelectric figure of merit (Z) for textured and reference specimens.

The ZT value of the undoped textured polycrystal is higher than that for Y-substituted $(ZnO)_5In_2O_3$ ceramics without preferred orientation.[13,14]

Texture engineering is an effective method for the enhancement of the thermoelectric properties of layer-structured materials. The thermoelectric properties of textured $(ZnO)_5In_2O_3$ ceramics could be further improved through appropriate doping or elemental substitution.

4 Conclusions

Textured bulk ceramics of the n-type thermoelectric oxide $(ZnO)_5In_2O_3$ were designed and fabricated by the use of plate-like $ZnSO_4{\cdot}3Zn(OH)_2$ particles as a reactive template. The textured $(ZnO)_5In_2O_3$, in spite of its low relative density (90%), exhibits in-plane electrical conductivity as high as full density non-oriented ceramics with the same composition. The low thermal conductivity of the textured $(ZnO)_5In_2O_3$ makes it a good thermoelectric material with a figure of merit nearly 3 times as large as that of the conventionally sintered non-textured specimen. The observed ZT value, 0.18 at 1073 K, is considered to be quite high for undoped n-type oxide polycrystals. The proposed processing method, reactive templated grain growth (RTGG), is an effective technique for the fabrication of textured ceramics with enhanced thermoelectric properties.

Acknowledgements

The authors are grateful to Dr N. Murayama and Dr W.-S. Shin of AIST for their kind cooperation in the laser flash measurement of thermal diffusivity. The authors would also like to thank Dr T. Yamamoto and Mr M. Toda of Hakusui Tech Co. for supplying precursor particles for ZnO.

References

1 H. Ohta, W.-S. Seo and K. Koumoto, *J. Am. Ceram. Soc.*, 1996, **79**, 2193.
2 M. Nakamura, N. Kimizuka and M. Mohri, *J. Solid State Chem.*, 1990, **86**, 16.
3 H. Hiramatsu, W.-S. Seo and K. Koumoto, *Chem. Mater.*, 1998, **10**, 3033.
4 H. Hiramatsu, H. Ohta, W.-S. Seo and K. Koumoto, *J. Jpn. Soc. Powder Powder Metall.*, 1997, **44**, 44.
5 T. Takenaka and K. Sakata, *Jpn. J. Appl. Phys.*, 1980, **19**, 31.
6 H. Igarashi, K. Matsunaga, T. Taniai and K. Okazaki, *Am. Ceram. Soc. Bull.*, 1978, **57**, 815.
7 H. Watanabe, T. Kimura and T. Yamaguchi, *J. Am. Ceram. Soc.*, 1991, **74**, 139.
8 T. Tani, *J. Korean Phys. Soc.*, 1998, **32**, S1217.
9 J. A. Horn, S. C. Zhang, U. Selvaraj, G. L. Messing and S. Trolier-McKinstry, *J. Am. Ceram. Soc.*, 1999, **82**, 921.
10 T. Takeuchi, T. Tani and Y. Saito, *Jpn. J. Appl. Phys.*, 1999, **38**, 5553.
11 T. Takeuchi, T. Tani and Y. Saito, *Jpn. J. Appl. Phys.*, 2000, **39**, 5577.
12 F. K. Lotgering, *J. Inorg. Nucl. Chem.*, 1959, **9**, 113.
13 M. Kazeoka, H. Hiramatsu, W.-S. Seo and K. Koumoto, *J. Mater. Res.*, 1998, **13**, 523.
14 M. Ohta, W.-S. Seo, W. Pitschke and K. Koumoto, *Key Eng. Mater.*, 1999, **71**, 169.